BMB Reports - Manuscript Submission

Manuscript Draft

Manuscript Number: BMB-22-089

Title: DN200434, an Orally Available Inverse Agonist of Estrogen-Related Receptor ɣ, Induces Ferroptosis in Sorafenib-Resistant Hepatocellular Carcinoma

Article Type: Article

Keywords: hepatocellular carcinoma; ERRɣ; DN200434; sorafenib; ferroptosis

Corresponding Author: Yeon-Kyung Choi

Authors: Dong-Ho Kim[1,#], Mi-Jin Kim[2,3,#], Na-Young Kim[3,#], Seunghyeong Lee[3], Jun-Kyu Byun[2,3], Jae Won Yun[4], Jaebon Lee[5], Jonghwa Jin[3], Jungwook Chin[6], Sung Jin Cho[7], In-Kyu Lee[1,2,3], Yeon-Kyung Choi[2,3,*], Keun-Gyu Park[1,2,3]

Institution: [1]Department of Biomedical Science and [2]Research Institute of Aging and Metabolism and [3]Department of Internal Medicine, Kyungpook National University,
[4]Veterans Medical Research Institute, Veterans Health Service Medical Center,
[5]School of Medicine, Sungkyunkwan University,
[6]New Drug Development Center, Daegu-Gyeongbuk Medical Innovation Foundation,

DN200434, an Orally Available Inverse Agonist of Estrogen-Related Receptor γ, Induces Ferroptosis in Sorafenib-Resistant Hepatocellular Carcinoma

Dong-Ho Kim[1,†], Mi-Jin Kim[2,3,†], Na-Young Kim[3,†], Seunghyeong Lee[3], Jun-Kyu Byun[2,3], Jae Won Yun[4], Jaebon Lee[5], Jonghwa Jin[3], Jungwook Chin[6], Sung Jin Cho[7], In-Kyu Lee[1,2,3], Yeon-Kyung Choi[2,3*], Keun-Gyu Park[1,2,3*]

[1]Department of Biomedical Science, Kyungpook National University, Daegu 41566, South Korea

[2]Research Institute of Aging and Metabolism, Kyungpook National University, Daegu 41566, South Korea

[3]Department of Internal Medicine, School of Medicine, Kyungpook National University, Kyungpook National University Hospital, Daegu, 41944, South Korea

[4]Veterans Medical Research Institute, Veterans Health Service Medical Center, Seoul 05368, South Korea

[5]Sungkyunkwan University School of Medicine, Seoul 16419, South Korea

[6]New Drug Development Center, Daegu-Gyeongbuk Medical Innovation Foundation, Daegu, 41061, South Korea

[7]Convergence Research Center for Diagnosis, Treatment and Care System of Dementia, Korea Institute of Science and Technology, Seoul 02792, South Korea

[†]These authors contributed equally

Running Title: DN200434 enhances ferroptosis by sorafenib in HCC

Keywords: hepatocellular carcinoma, ERRγ, DN200434, sorafenib, ferroptosis

*Corresponding authors' address: Department of Internal Medicine, School of Medicine, Kyungpook National University, Kyungpook National University Hospital, Daegu, Korea (K-G Park and Y-K Choi); E-mail addresses and Tel.: kpark@knu.ac.kr, +82-53-200-5505 (K-G Park), ykchoi@knu.ac.kr +82-53-200-3869 (Y-K Choi)

ABSTRACT

Sorafenib, originally identified as an inhibitor of multiple oncogenic kinases, induces ferroptosis in hepatocellular carcinoma (HCC) cells. Several pathways that mitigate sorafenib-induced ferroptosis confer drug resistance; thus strategies that enhance ferroptosis increase sorafenib efficacy. Orphan nuclear receptor estrogen-related receptor γ (ERRγ) is upregulated in human HCC tissues and plays a role in cancer cell proliferation. The aim of this study was to determine whether inhibition of ERRγ with DN200434, an orally available inverse agonist, can overcome resistance to sorafenib through induction of ferroptosis. Sorafenib-resistant HCC cells were less sensitive to sorafenib-induced ferroptosis and showed significantly higher ERRγ levels than sorafenib-sensitive HCC cells. DN200434 induced lipid peroxidation and ferroptosis in sorafenib-resistant HCC cells. Mechanistically, DN200434 increased mitochondrial ROS generation by reducing glutathione/glutathione disulfide levels, which subsequently reduced mTOR activity and GPX4 levels. DN200434-induced amplification of the antitumor effects of sorafenib was confirmed in a tumor xenograft model. The present results indicate that DN200434 may be a novel therapeutic strategy to re-sensitize HCC cells to sorafenib.

INTRODUCTION

Sorafenib, an oral multi-kinase inhibitor, is a first-generation targeted therapy that has demonstrated survival benefits in patients with advanced HCC (1, 2). Despite recent advances in immunomodulating therapies for HCC, sorafenib remains the most effective single drug for monotherapy (3). However, the majority of patients develop drug resistance within approximately 6 months of starting treatment (4). Thus, combination treatment with different drugs is considered to be a potential approach to improving the antitumor effects of sorafenib (5, 6).

Ferroptosis is an iron-dependent form of cell death characterized by increased production of reactive oxygen species (ROS) via the Fenton reaction, as well as accumulation of lipid peroxidation products (7). Ferroptosis is induced by inhibiting the cystine-glutamate antiporters Xc- or xCT, which import cystine for *de novo* synthesis of the important antioxidant peptide glutathione. Accumulating evidence shows that sorafenib induces ferroptosis by inhibiting cysteine uptake; therefore, pathways that mitigate sorafenib-induced ferroptosis induce drug resistance (8, 9). Recently, the challenges of inducing ferroptosis have attracted attention as a potent therapeutic strategy to reverse cancer resistance to sorafenib.

The orphan nuclear receptor estrogen-related receptor (ERR)γ plays an important role in mitochondrial metabolism and redox balance in tissues that have high metabolic demand, including heart, skeletal muscle, liver, and brown adipose tissue (10). ERRγ is also closely related to progression of breast cancer and anaplastic thyroid cancer (11, 12). Singh et al. suggested the potential clinical applicability of ERRγ inhibition by DN200434, an orally bioavailable and highly selective ERRγ inverse agonist, for the treatment of anaplastic thyroid

cancer (12). Previously, we reported that ERRγ has clinical significance with respect to the diagnosis and treatment of HCC (13). However, the role of ERRγ as a modulator of ferroptosis in sorafenib resistance remains unclear.

Here, we examined whether ERRγ is involved in sorafenib resistance of HCC, and whether the ERRγ inverse agonist DN200434 induces ferroptosis and re-sensitizes sorafenib-resistant HCC to sorafenib.

RESULTS

Sorafenib-resistant HCC cells overexpress ERRγ and fail to induce ferroptosis

Sorafenib-resistant Huh7 and SK-Hep1 cells were established as previously described (14). As shown in Figure 1A, sorafenib-resistant Huh7 and SK-Hep1 cells became less sensitive to sorafenib over time, or when exposed to different concentrations for 24 h. To determine whether sorafenib induces ferroptosis in HCC, we monitored lipid ROS accumulation, which is a hallmark of ferroptosis, using C11-BODIPY. As expected, treatment with sorafenib increased lipid peroxidation in sorafenib-sensitive HCC cells but not in sorafenib-resistant HCC cells (Figure 1B). The publicly available gene dataset GSE73571 was extracted from the Gene Expression Omnibus (GEO) database to obtain data on the phenotypes of four sorafenib-acquired resistant and three sorafenib-sensitive HCC cells. Analysis of this dataset showed that sorafenib treatment significantly increases ERRγ levels in HCC cells (Figure 1C). Also, the data suggest that ERRγ levels are significantly higher in sorafenib-resistant HCC cells than in sorafenib-sensitive HCC cells, suggesting that ERRγ is involved in sorafenib resistance (Figure 1D and E).

DN200434 enhances sorafenib-induced ferroptosis in sorafenib-resistant HCC cells

Given the upregulation of ERRγ and the failure of ferroptosis induction in sorafenib-resistant HCC cells, we next explored whether inhibiting ERRγ sensitizes sorafenib-resistant HCC cells through recovery of ferroptosis. To this end, we first confirmed that ERRγ protein levels in sorafenib-resistant HCC cells were downregulated by DN200434, which is already known to significantly decrease endogenous ERRγ expression in CAL62 cells (12) (Figure 2A). Next,

we assessed accumulation of lipid ROS in sorafenib-resistant HCC cells in the presence/absence of DN200434. We found that sorafenib or DN200434 alone did not increase accumulation of lipid ROS in sorafenib-resistant HCC cells, whereas a combination of sorafenib and DN200434 induced ferroptosis, as evidenced by increased lipid peroxidation and 4-HNE staining intensity (Figure 2B–E). In parallel with ferroptosis induction, sorafenib-resistant HCC cell death assessed by the LDH release assay was increased more by combined treatment with sorafenib and DN200434 than by sorafenib or DN200434 treatment alone; this was prevented by the presence of ferrostatin-1 (Figure 2F). Given that sorafenib or DN200434 alone did not increase ferroptosis or cell death in sorafenib-resistant HCC cells, these findings indicate that, rather than by acting synergistically with sorafenib in sorafenib-resistant HCC cells, DN200434 renders sorafenib-resistant HCC cells more susceptible to ferroptosis.

DN200434 increases mitochondrial ROS, and downregulates mTORC1 activity and GPX4 levels

ERRγ is involved in mitochondrial homeostasis (15); therefore, we investigated whether induction of DN200434-mediated ferroptosis was associated with mitochondrial ROS production. As shown in Figure 3A and B, sorafenib or DN200434 alone did not increase the amount of mitochondrial-derived superoxide stained by MitoSOX; however, the combination of sorafenib and DN200434 increased mitochondrial ROS significantly in sorafenib-resistant HCC cells (Figure 3A and B). Based on previous results showing a higher glutathione (GSH)/ glutathione disulfide (GSSG) ratio in sorafenib-resistant HCC cells (14), we measured the GSH/GSSG ratio in sorafenib-resistant cells in the absence/presence of DN200434. As shown

in Figure 3C, sorafenib or DN200434 alone did not alter the GSH/GSSG ratio; however, the combination of DN200434 and sorafenib decreased the GSH/GSSG ratio in sorafenib-resistant HCC cells significantly, compared with sorafenib or DN200434 treatment alone (Figure 3C). Glutathione peroxidase-4 (GPX4) is the key upstream regulator of ferroptosis (7). Given that mitochondrial ROS reduces mTORC1 (16, 17), and that mTORC1 protects against ferroptosis by promoting GPX4 protein synthesis (18), we investigated the effects of DN200434 on mTORC1 activity and GPX4 levels in sorafenib-resistant HCC cells. Co-treatment of sorafenib-resistant HCC cells with DN200434 and sorafenib decreased mTORC1 activity, as measured by detection of phosphorylated mTOR (Ser-2448) and 4E binding protein 1(4E-BP1), and GPX4 levels, whereas this was not observed in the group treated with sorafenib or DN200434 alone (Figure 3D). Notably, supplementation with GSH reversed the increase in mitochondrial ROS and decrease in mTORC1 activity and GPX4 levels induced by combined treatment of sorafenib-resistant HCC cells with sorafenib and DN200434 (Figure 3A, B, and D). In accordance with these results, and as shown in Figure 2F, the increase in HCC cell death in the presence of DN200434 and sorafenib was reversed significantly when ferroptosis was inhibited by GSH. Collectively, these findings indicate that DN200434 potentiates ferroptosis via mitochondrial ROS-induced inhibition of mTORC1 and GPX4, thereby improving the response of sorafenib-resistant HCC cells to sorafenib.

Effect of DN200434 on tumor growth in a sorafenib-resistant HCC xenograft model

Finally, we examined the effect of DN200434 on tumor growth in nude mice bearing subcutaneous sorafenib-resistant Huh7 and SK-Hep1 xenografts. Tumors were significantly

larger in mice injected with Huh7 SR than in mice injected with Huh7 SS (Figure 4A). The reduction in tumor growth in mice treated with sorafenib plus DN200434 was greater than that in mice treated with sorafenib alone, with no difference in body weight between the groups (Figure 4B–D). The efficiency of combined treatment with sorafenib and DN200434 on tumor growth was confirmed in nude mice bearing sorafenib-resistant SK-Hep1 cells (Figure 4E–H).

DISCUSSION

In the present study, we showed that ERRγ is markedly upregulated in sorafenib-resistant HCC cells, and that inhibition of ERRγ by DN200434 increases their susceptibility to sorafenib. Co-treatment with DN200434 and sorafenib significantly increased mitochondrial ROS, while at the same time decreasing mTORC1 activity and GPX4 levels, thereby potentiating sorafenib-induced ferroptosis in HCC cells. The efficacy of combined treatment with DN200434 and sorafenib was confirmed in xenograft models.

Previously, we reported that the degree of ERRγ expression in surgically resected human HCC tissues is associated with advanced clinical stage and invasive pathologic grade (13), and provided a rationale for ERRγ as a possible therapeutic target for HCC by showing that an ERRγ inverse agonist-induced ROS generation and suppressed HCC cell proliferation (13). Here, analysis of the data from sorafenib-resistant HCC cells and the Gene expression Omnibus (GEO) database revealed that ERRγ is also overexpressed in sorafenib resistance in HCC cells and tissues, suggesting that ERRγ plays a role in the development of sorafenib resistance. During oxidative remodeling, ERRγ plays an essential role in supporting mitochondrial metabolic fitness by driving a transcriptional network that activates mitochondrial biogenesis,

oxidative phosphorylation, and the electron transport chain in various cellular processes (15). Tissue-specific deletion of ERRγ results in a reduced oxygen consumption rate and elevated mitochondrial ROS production (19, 20). Consistent with these findings, we showed herein that inhibition of ERRγ by DN200434 increased mitochondrial ROS, supporting the hypothesis that ERRγ is implicated in drug resistance through impaired mitochondrial function.

Growing evidence shows that changes in cellular metabolism, redox homeostasis, and various signaling pathways are involved in regulating cell sensitivity to ferroptosis (18, 21). Recent findings demonstrate that mTORC1, a central controller of cell growth and metabolism, is a regulator of ferroptosis (18, 22). Inactivation of mTORC1 by PI3K/AKT inhibitors or mTOR inhibitors suppresses synthesis of GPX4 protein, which plays a crucial role in protection against ferroptosis, via downstream 4EBP; this triggers autophagy and sensitizes cells to lipid peroxidation and ferroptosis (22, 23). The work presented herein shows that mTORC1 activity in sorafenib-resistant HCC cells was decreased by combined treatment with DN200434 and sorafenib, which is consistent with previous reports showing that mitochondrial ROS reduce mTORC1 (16, 17). Notably, co-treatment with DN200434 and sorafenib suppressed mTORC1 activity and GPX4 levels. When combined with results showing that co-treatment with DN200434 and sorafenib leads to significant tumor regression *in vitro* and *in vivo*, these findings indicate that DN200434 improves the response to sorafenib by enhancing ferroptosis.

In conclusion, we showed that ERRγ contributes to the resistance to sorafenib, and that inhibition of ERRγ with DN200434 recovers sorafenib sensitivity by inducing ferroptosis. Our findings further emphasize that DN200434 may be a useful adjuvant agent in new treatment protocols aimed at increasing the susceptibility of HCC to sorafenib.

MATERIALS AND METHODS

Cell culture and chemical treatments

Human HCC Huh7 and SK-Hep1 cells were obtained from the American Type Culture Collection (Manassas, VA, USA). To generate sorafenib-resistant HCC cells (Huh7 (SR) and SK-Hep1 (SR)), Huh7 and SK-Hep1 cells were cultured in the presence of increasing concentrations (up to a maximum concentration of 10 μM) of sorafenib (Cayman Chemical, Ann Arbor, MI, USA) for 8 months, as previously described (14 Sorafenib-resistant HCC cells (Huh7 (SR) and SK-Hep1 (SR) cells) and their parenteral cells (Huh7 and SK-Hep1 cells) were cultured in Dulbecco's modified Eagle's medium (Biological Industries, Kibbutz Beit Haemek, Israel) supplemented with 10% fetal bovine serum (FBS) and 1% penicillin/streptomycin. Sorafenib-resistant HCC cells and their parenteral cells were seeded at $3–5\times10^3$ cells per well in 96-well plates. The cells were serum-starved for 24 h and incubated with 10% FBS with or without sorafenib for 24 h, and cell viability was measured using CCK8 Solution Reagent (CK04; Dojindo). The absorbance of each well at 495 nm was measured on a VERSA MAX ELISA reader (Molecular Devices). The proportion of viable cells in each treatment group was normalized against that in control wells. To determine the effects of ferroptosis on HCC cells, cells were treated with 10 μM sorafenib (Cayman), 12 μM DN200434, 1 μM ferrostatin-1 (Sigma, St. Louis, MO, USA), or 2 mM glutathione reduced-ethyl ester (Sigma) for 24 h.

Detection of lipid ROS

For fluorescence detection of lipid ROS, cells were stained for 30 minutes with C11-BODIPY (10 μM; Thermo Fisher Scientific) and washed three times with PBS, and the nuclei were

stained using NucBlueTM Live ReadyProbesTM Reagent (Thermo Fisher Scientific). Data were presented as the ratio of the intensity of green/red fluorescence in cells. For 4-HNE staining, cells on glass slides were fixed for 15 min in 4% paraformaldehyde and then permeabilized with 0.3% Triton X-100 for 10 min at room temperature. Following 1 h of blocking in 5% normal goat serum (Vector Laboratories, Burlingame, USA), cells were incubated overnight at 4°C with a primary anti-4-HNE (Abcam, 1:100) antibody. After washing, the cells were incubated for 1 h at room temperature with an Alexa Fluor™ 568 goat-anti-rabbit (Thermo Fisher Scientific) secondary antibody. Nuclei were stained with DAPI (Vector Laboratories). Fluorescence intensity was determined by obtaining the integrated signal density/cell.

Lactate dehydrogenase release assay

Cells were seeded at 1 × 10^4/well into a 96-well plates and incubated at the indicated concentrations in cell culture medium for 24 h at 37°C. LDH release into the medium was detected using the LDH-Glo™ Cytotoxicity Assay (Promega, Madison WI, USA), as recommended by the manufacturer. The release of LDH from untreated cells was used as a control.

Immunoblot analysis

Cells were incubated on ice for 30 min in IPH lysis buffer (50 mM Tris [pH 8.0], 150 mM NaCl, 5 mM EDTA, 0.1 mM phenylmethylsulphonyl fluoride [PMSF], and 0.5% NP-40)

containing a protease inhibitor cocktail (Sigma) and dithiothreitol. Lysates were clarified by centrifugation at 12,000 × g for 10 min. Supernatants were collected, and the protein concentration was measured using the Bio-Rad protein assay (Bio-Rad, Richmond, CA, USA). Proteins in cell lysates were separated by SDS-PAGE and transferred to PVDF membranes (Millipore Corporation, Bedford, MA, USA). The membranes were incubated with primary antibodies specific for the following proteins: phospho-mTOR (S2448), mTOR, phospho-4E-BP1, 4E-BP1, GPX4 (Cell Signaling Technology), and actin (Sigma). After three washes in TBST, membranes were incubated with horseradish peroxidase-conjugated secondary antibodies (Santa Cruz Biotechnology, Santa Cruz, CA, USA). Immunoreactive proteins were visualized by chemiluminescence (UVITec, Cambridge, UK).

Quantitative RT-PCR

Total RNA was prepared using the QIAzol lysis reagent (Qiagen, Hilden, Germany), and cDNA was synthesized using the RevertAid First Strand cDNA Synthesis kit (Thermo Fisher Scientific, Inc.). The resultant cDNA was amplified on a 7500 Fast Real-Time PCR System (Applied Biosystems, Foster City, CA, USA). Gene expression was normalized to that of the corresponding level of β-actin mRNA. The primer sequences were as follows: ERRγ forward, CGATGCCCAAGAGACTGTGTT; reverse, AGACGCACCCCTTCTTTCAG.

GEO data processing

The gene expression profile dataset GSE73571 was downloaded from the Gene expression Omnibus (GEO) database (http://www.ncbi.nlm.nih.gov/gds/). R 3.6.3 (R Core Team;

Auckland, New Zealand) was used for statistical analysis and to calculate fold-changes between sorafenib-sensitive and sorafenib-resistant tumors.

Measurement of the GSH/GSSG ratio

Cells were seeded at 1 × 10^4/well in a 96-well plate and incubated at the indicated concentrations in cell culture medium for 24 h at 37°C. The experiments were repeated independently three times. Briefly, to measure the glutathione (GSH)/ glutathione disulfide (GSSG) ratio, the GSH/GSSG-Glo™ Assay (Promega) was performed according to the manufacturer's protocol using 50 µL per well of total glutathione lysis reagent or oxidized glutathione lysis reagent. A vehicle control (cells incubated with DMSO) and a no-cell control (PBS) were also included. The glutathione concentrations (µM) were determined in the final reaction volume (200 µL), and the GSH/GSSG ratio was calculated using the following equation: Total GSH RLU × GSSG RLU)/GSSG RLU.

MitoSox

Mitochondrial ROS generation was assessed using the MitoSOX Red Mitochondrial Superoxide indicator (Invitrogen, Carlsbad, CA, USA). Huh7 (SR) and SK-Hep1 (SR) cells on a confocal dish were treated with 10 µM sorafenib in the presence/absence of 12 µM DN200434 for 24 h. Cells were then treated with 5 µM MitoSOX reagent working solution and incubated for 10 min at 37°C in the dark. The cells were then washed gently three times with warm HBSS buffer. Finally, cells were counterstained with NucBlue Live Cell Stain

ReadyProbes (Invitrogen) and mounted in warm buffer for imaging. MitoSOX fluorescence intensity was quantified using ImageJ software.

Animal experiments

Huh7 (SR) or SK-Hep1 (SR) cells (6×10^6), and Huh7 (SS) or SK-Hep1 (SS) cells (6×10^6), were injected subcutaneously into the right flank of 6-week-old athymic male BALB/c nude (nu/nu) mice. Mice were randomized into three groups (n = 5 in the Huh7/Huh7 (SR) group and n=4 in the SK-Hep1/SK-Hep1 (SR) group, respectively). When the tumor volume was around 100 mm3, mice received sorafenib (10 mg/kg via i.p. injection), DN200434 (10 mg/kg via oral gavage), or vehicle control (DMSO in PBS) every day for 15 days. Tumors were measured every 3 days using calipers and the volume was calculated as length × width2 × 0.5 (mm3). All animal procedures were approved by the Institutional Animal Care and Use Committee of Kyungpook National University School of Medicine (KNU-2018-0015 and KNU-2021-0001).

Statistical analysis

Data were expressed as the mean ± standard error of the mean (SEM) of at least three independent experiments. Statistical difference was determined by Student's t-test (Prism software); a p value < 0.05 was considered statistically significant.

ACKNOWLEDGMENTS

This work was supported by National Research Foundation of Korea (NRF) grants NRF-2021R1A2C3005603, NRF-2017M3A9G7073086, 2022R1A2C1008591, and NRF-2020R1A5A2017323, funded by the Ministry of Science and the ICT; and by grant HI16C1501 from the Korea Health Technology R&D Project through the Korea Health Industry Development Institute, funded by the Ministry of Health and Welfare.

CONFLICTS OF INTEREST

The authors declare no conflicts of interest regarding this manuscript.

FIGURES and LEGENDS

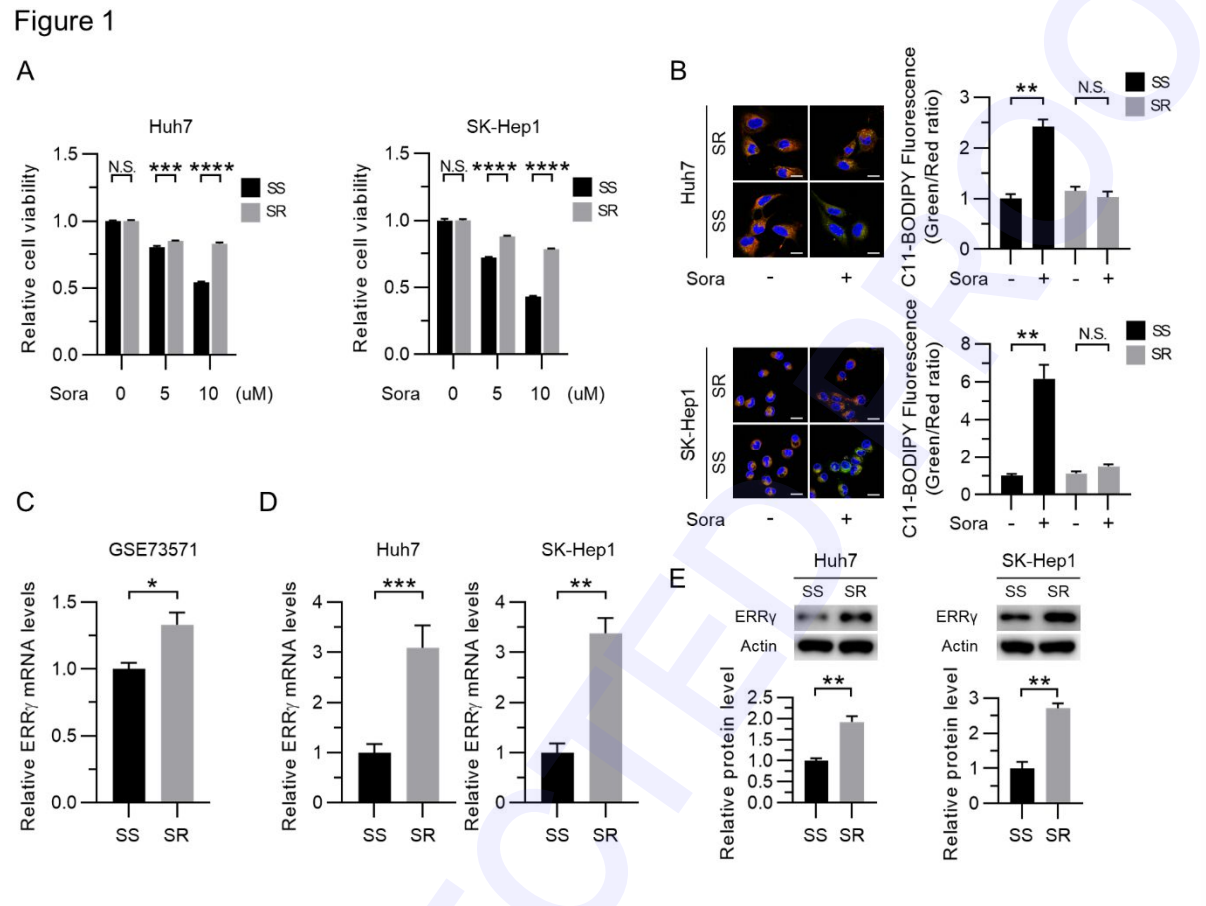

Figure 1. Sorafenib-resistant HCC cells show higher ERRγ expression and are less sensitive to sorafenib-induced ferroptosis. (A) Sorafenib-sensitive (SS) and -resistant (SR) HCC (Huh7 and SK-Hep1) cells were treated with the indicated concentrations of sorafenib for 24 h and cell viability was assayed using the CCK-8 assay. (B) Representative images of C11-BODIPY, a marker of lipid peroxidation, in sorafenib-resistant (SR) HCC cells, and in parental cells (SS) treated with sorafenib (left panel). Quantification of C11-BODIPY fluorescence in cells (right panel). (C) Relative expression of ERRγ mRNA in sorafenib-resistant HCC cells (data from the GEO database). (D) Relative expression of ERRγ mRNA levels in sorafenib-sensitive (SS) and -resistant (SR) HCC cells. (E) Representative western

blot analysis of ERRγ protein levels in sorafenib-sensitive (SS) and -resistant (SR) HCC cells. Data in the bar graph are mean ± SEM of three independent experiments. N.S., not significant; *p < 0.05, **p < 0.01, ***p < 0.001, and ****p < 0.0001. Sora, Sorafenib.

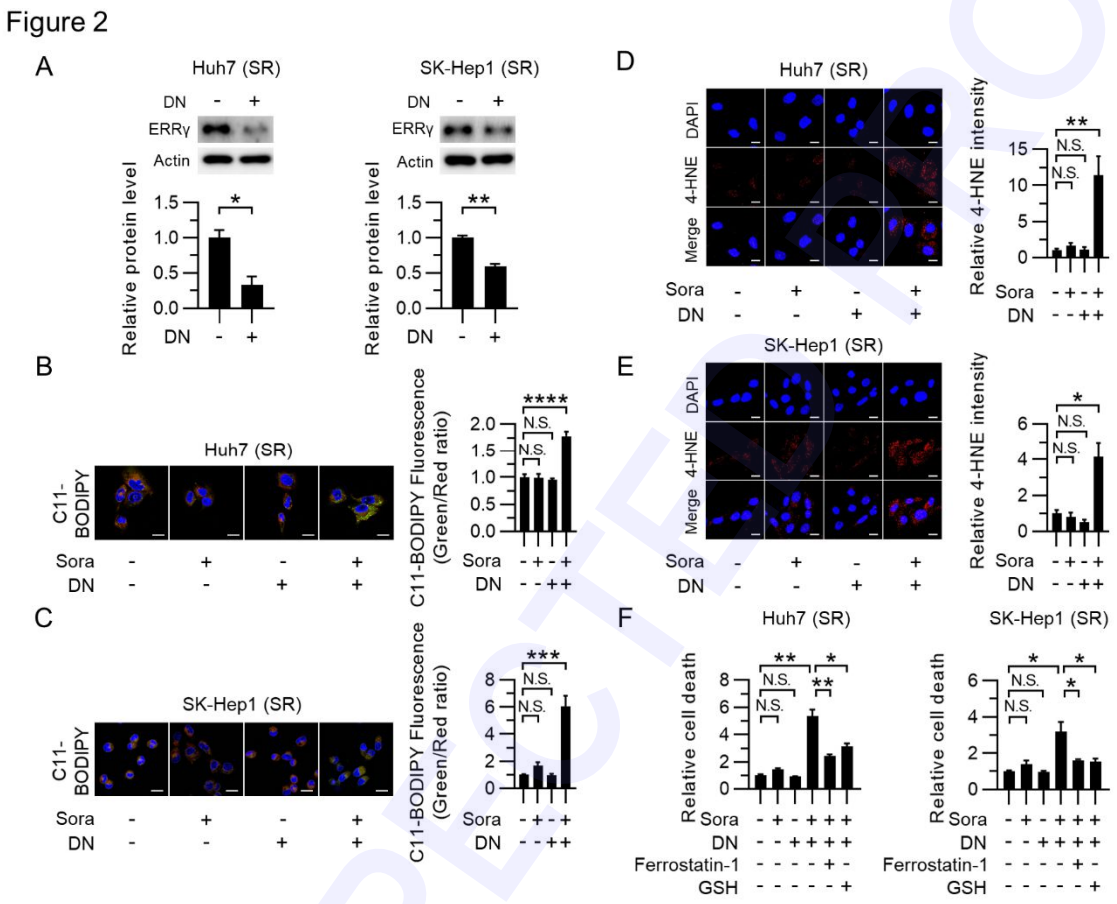

Figure 2. Inhibition of ERRγ by DN200434 sensitizes sorafenib-resistant HCC cells to ferroptosis. (A) Representative western blot analysis of ERRγ protein levels in sorafenib-resistant (SR) Huh7 (left panel) and SK-Hep1 cells (right panel) in the presence/absence of DN200434. (B and C) Representative images of C11-BODIPY and quantification of C11-BODIPY fluorescence in sorafenib-resistant (SR) Huh7 (B) and SK-Hep1 (C) cells treated with sorafenib or DN200434. Quantification of C11-BODIPY fluorescence in cells. (D and E) Representative immunofluorescence staining with anti-4-HNE, and quantification of 4-HNE

fluorescence in sorafenib-resistant (SR) Huh7 (D) and SK-Hep1 (E) cells treated with sorafenib or DN200434. (F) Relative cell death of sorafenib-resistant (SR) Huh7 (left panel) and SK-Hep1 cells (right panel). Cell death was assessed by LDH release after treatment for 24 h with sorafenib or DN200434 in the presence/absence of ferrostatin-1 or GSH. Scale bar, 20 μm. Data are expressed as the mean ± SEM of three independent experiments. N.S., not significant; *$p < 0.05$, **$p < 0.01$, ***$p < 0.001$, and ****$p < 0.0001$. Sora, Sorafenib; DN, DN200434.

Figure 3

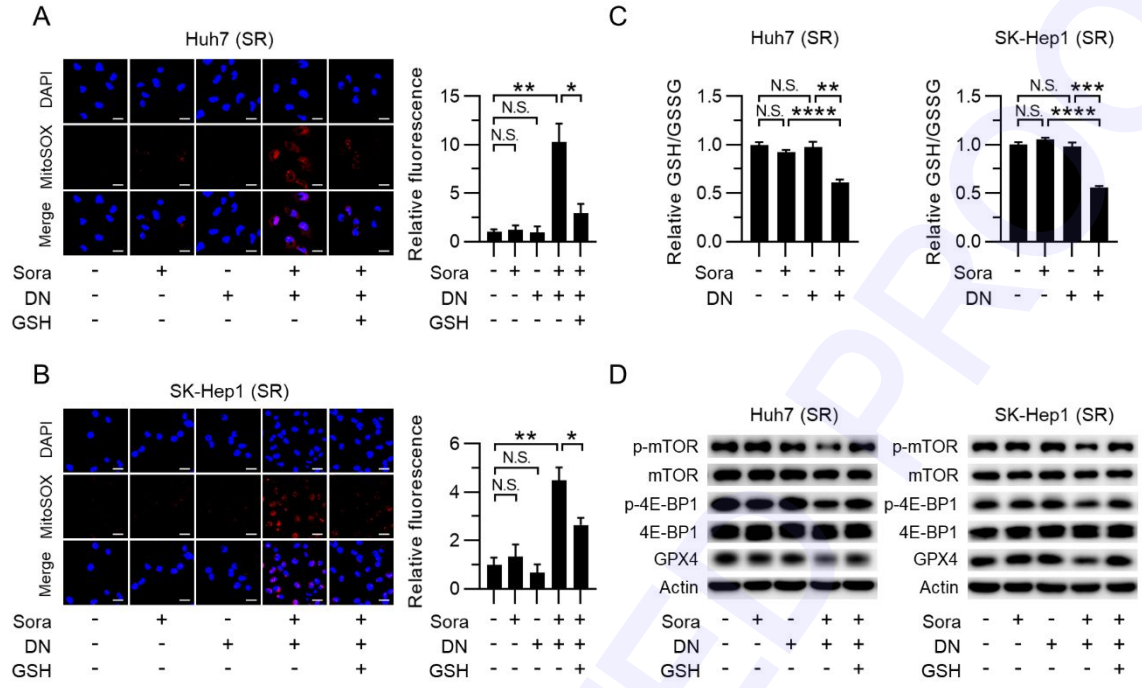

Figure 3. The ERRγ inverse agonist DN200434 increases mitoROS levels, and decreases mTORC1 activity and GPX4 protein levels.

(A and B) Representative fluorescence images showing mitochondrial superoxide production in sorafenib-resistant (SR) Huh7 (A) and SK-Hep1 (B) cells. The bar graph shows quantification of MitoSOX fluorescence intensity (red) and nuclear counterstaining with DAPI (blue). (C) Measurement of relative GSH/GSSG ratios in sorafenib-resistant (SR) Huh7 and SK-Hep1 cells. (D) Levels of phosphorylated mTOR, phosphorylated 4E-BP1, and GPX4 in sorafenib-resistant (SR) Huh7 and SK-Hep1 cells treated with sorafenib or DN200434 in the presence/absence of GSH. Scale bar, 20 μm. Data are expressed as the mean ± SEM of three independent experiments. N.S., not significant; *$p < 0.05$, **$p < 0.01$, ***$p < 0.001$, and ****$p < 0.0001$. Sora, Sorafenib; DN, DN200434.

Figure 4

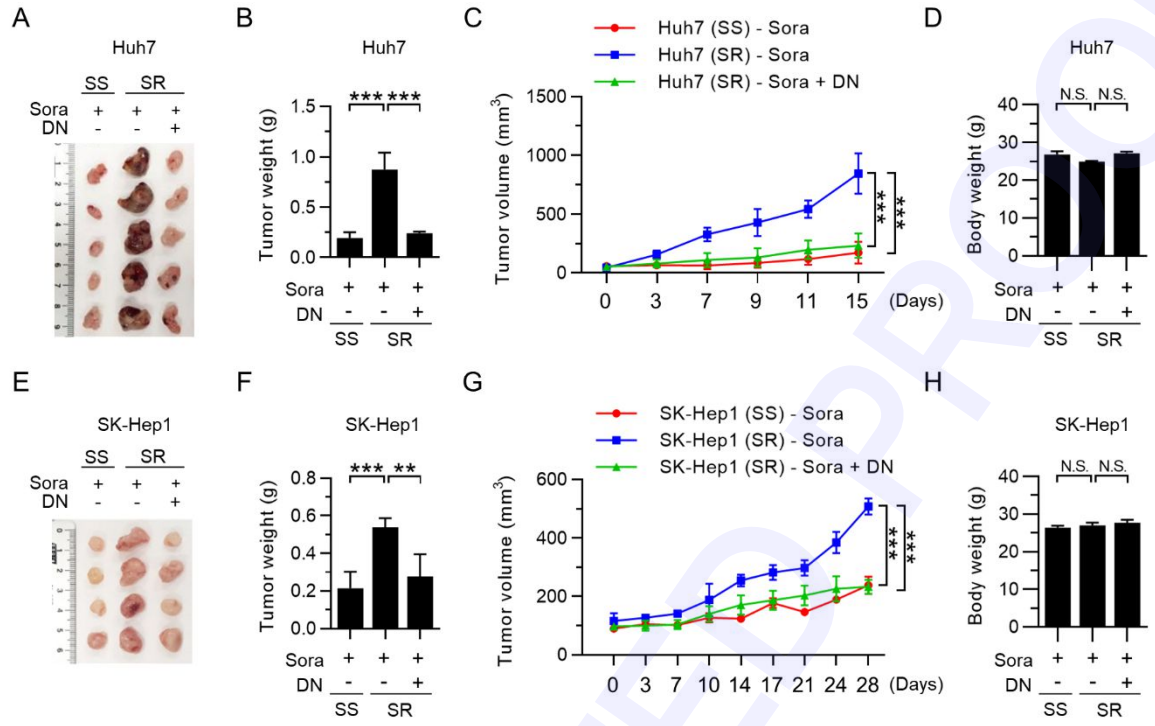

Figure 4. Effect of DN200434 on tumor growth in a sorafenib-resistant HCC xenograft model.

(A–D) Representative images of an excised tumor (A), tumor weight (B), tumor volume (C), and body weight (D) of mice treated with sorafenib (10 mg/kg) in the presence/absence of DN200434 (10 mg/kg). Sorafenib-sensitive (SS) or –resistant (SR) Huh7 cells (6×10^6) cells were injected subcutaneously into the right flank of each mouse. Data are expressed as the mean ± SEM (n = 5 per group). (E–H) Representative image of excised tumor xenografts (E), tumor weight (F), tumor volume (G), and body weight (H) of mice treated with sorafenib (10 mg/kg) in the presence/absence of DN200434 (10 mg/kg). Sorafenib-sensitive (SS) or -resistant (SR) cells (6×10^6) were injected subcutaneously into the right flank of each mouse. Data are expressed as the mean ± SEM (n = 4 per group). N.S., not significant; **p < 0.01 and ***p < 0.001. Sora, Sorafenib; DN, DN200434.

References

1. Llovet JM, Zucman-Rossi J, Pikarsky E et al (2016) Hepatocellular carcinoma. Nat Rev Dis Primers 2, 16018
2. Kudo M, Finn RS, Qin S et al (2018) Lenvatinib versus sorafenib in first-line treatment of patients with unresectable hepatocellular carcinoma: a randomised phase 3 non-inferiority trial. Lancet 391, 1163-1173
3. Llovet JM, Kelley RK, Villanueva A et al (2021) Hepatocellular carcinoma. Nat Rev Dis Primers 7, 6
4. Abdel-Rahman O, Abdel-Wahab M, Shaker M, Abdel-Wahab S, Elbassiony M and Ellithy M (2013) Sorafenib versus capecitabine in the management of advanced hepatocellular carcinoma. Med Oncol 30, 655
5. Samalin E, Bouche O, Thezenas S et al (2014) Sorafenib and irinotecan (NEXIRI) as second- or later-line treatment for patients with metastatic colorectal cancer and KRAS-mutated tumours: a multicentre Phase I/II trial. Br J Cancer 110, 1148-1154
6. Zhu AX, Stuart K, Blaszkowsky LS et al (2007) Phase 2 study of cetuximab in patients with advanced hepatocellular carcinoma. Cancer 110, 581-589
7. Li J, Cao F, Yin HL et al (2020) Ferroptosis: past, present and future. Cell Death Dis 11, 88
8. Byun JK, Lee S, Kang GW et al (2022) Macropinocytosis is an alternative pathway of cysteine acquisition and mitigates sorafenib-induced ferroptosis in hepatocellular carcinoma. J Exp Clin Cancer Res 41, 98
9. Sun X, Niu X, Chen R et al (2016) Metallothionein-1G facilitates sorafenib resistance through inhibition of ferroptosis. Hepatology 64, 488-500
10. Bookout AL, Jeong Y, Downes M, Yu RT, Evans RM and Mangelsdorf DJ (2006) Anatomical profiling of nuclear receptor expression reveals a hierarchical transcriptional network. Cell 126, 789-799
11. Ariazi EA, Clark GM and Mertz JE (2002) Estrogen-related receptor alpha and estrogen-related receptor gamma associate with unfavorable and favorable biomarkers, respectively, in human breast cancer. Cancer Res 62, 6510-6518
12. Singh TD, Song J, Kim J et al (2019) A Novel Orally Active Inverse Agonist of Estrogen-related Receptor Gamma (ERRgamma), DN200434, A Booster of NIS in Anaplastic Thyroid Cancer. Clin Cancer Res 25, 5069-5081
13. Kim JH, Choi YK, Byun JK et al (2016) Estrogen-related receptor gamma is upregulated in liver cancer and its inhibition suppresses liver cancer cell proliferation via induction of p21 and p27. Exp Mol Med 48, e213
14. Kim MJ, Choi YK, Park SY et al (2017) PPARdelta Reprograms Glutamine Metabolism in Sorafenib-Resistant HCC. Mol Cancer Res 15, 1230-1242
15. Alaynick WA (2008) Nuclear receptors, mitochondria and lipid metabolism. Mitochondrion 8, 329-337
16. Li ZY, Yang Y, Ming M and Liu B (2011) Mitochondrial ROS generation for regulation of autophagic pathways in cancer. Biochem Biophys Res Commun 414, 5-8
17. Ni HM, Williams JA, Jaeschke H and Ding WX (2013) Zonated induction of autophagy and mitochondrial spheroids limits acetaminophen-induced necrosis in the liver. Redox Biol 1, 427-432
18. Lei G, Zhuang L and Gan B (2021) mTORC1 and ferroptosis: Regulatory mechanisms and therapeutic potential. Bioessays 43, e2100093

19. Li W, Gong M, Park YP et al (2021) Lupus susceptibility gene Esrrg modulates regulatory T cells through mitochondrial metabolism. JCI Insight 6
20. Fan W, He N, Lin CS et al (2018) ERRgamma Promotes Angiogenesis, Mitochondrial Biogenesis, and Oxidative Remodeling in PGC1alpha/beta-Deficient Muscle. Cell Rep 22, 2521-2529
21. Zhang Y, Swanda RV, Nie L et al (2021) mTORC1 couples cyst(e)ine availability with GPX4 protein synthesis and ferroptosis regulation. Nat Commun 12, 1589
22. Yi J, Zhu J, Wu J, Thompson CB and Jiang X (2020) Oncogenic activation of PI3K-AKT-mTOR signaling suppresses ferroptosis via SREBP-mediated lipogenesis. Proc Natl Acad Sci U S A 117, 31189-31197
23. Liu Y, Wang Y, Liu J, Kang R and Tang D (2021) Interplay between MTOR and GPX4 signaling modulates autophagy-dependent ferroptotic cancer cell death. Cancer Gene Ther 28, 55-63

Figure 1

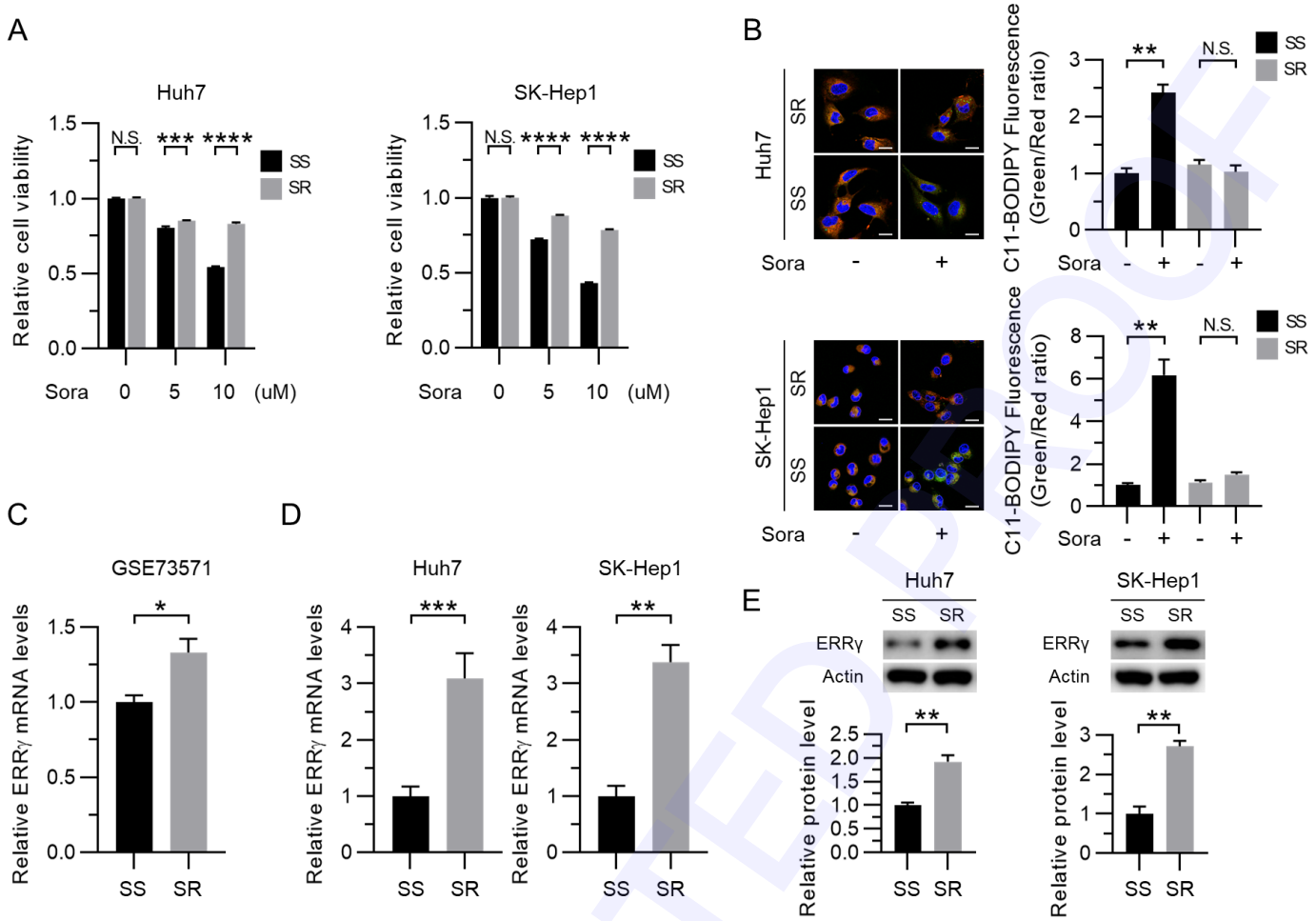

Fig. 1. Revised Figure 1

Figure 2

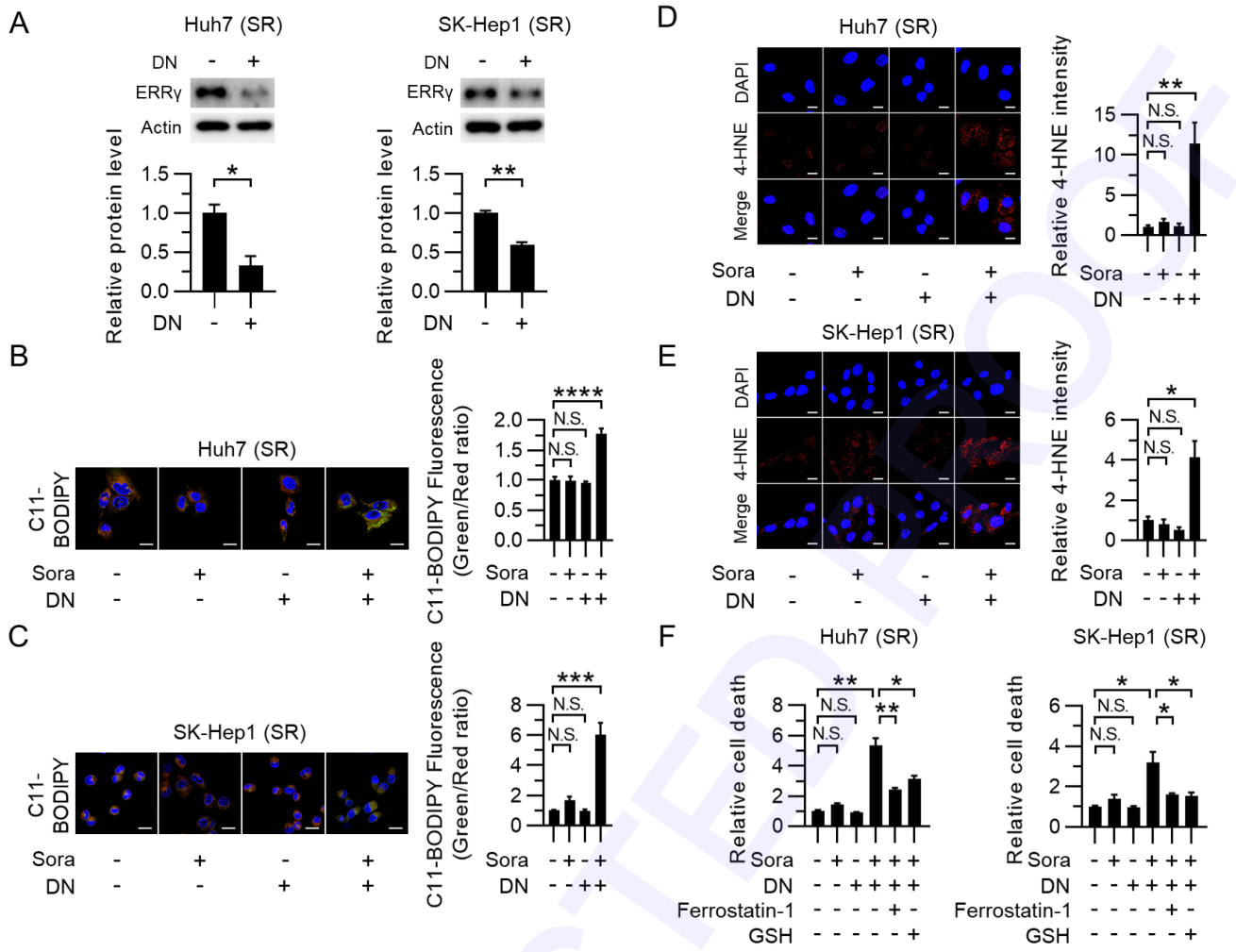

Fig. 2. Revised Figure 2

Figure 3

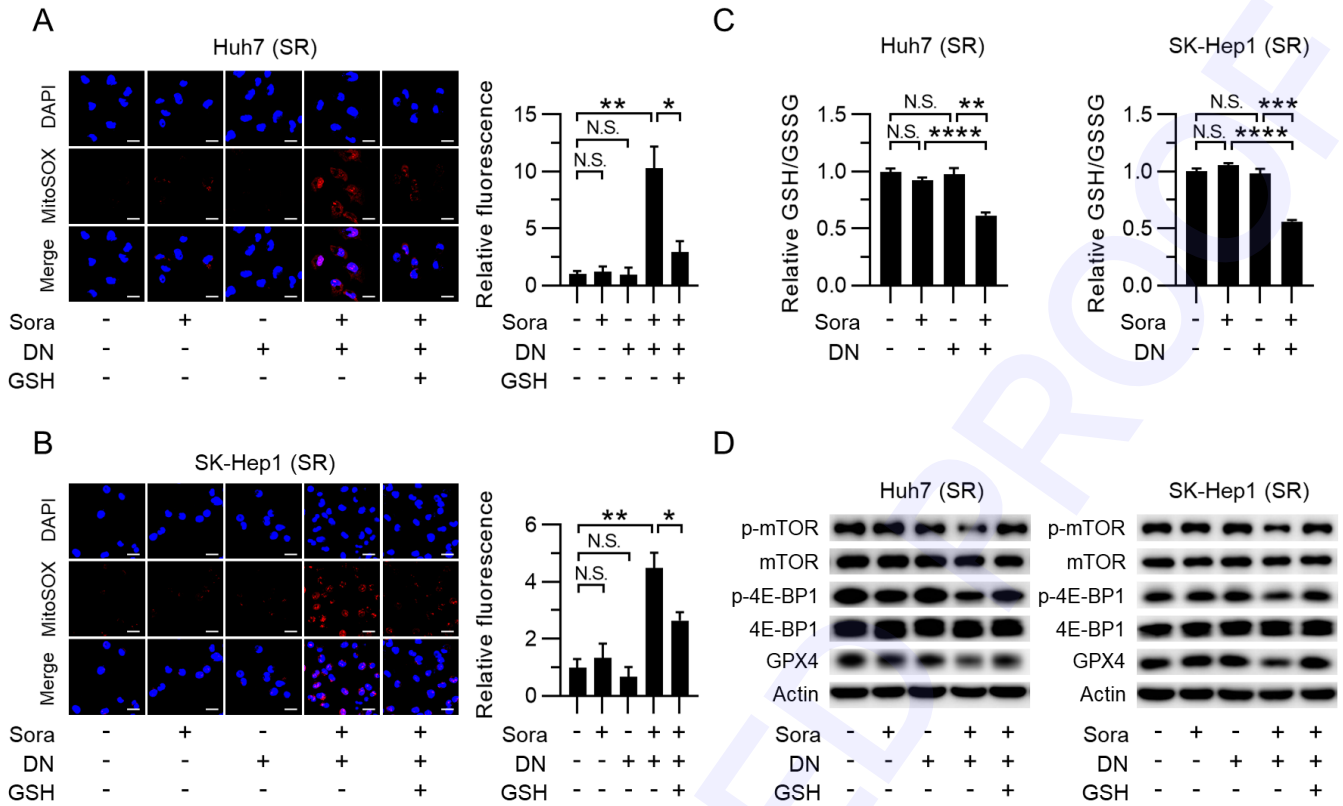

Fig. 3. Revised Figure 3

Figure 4

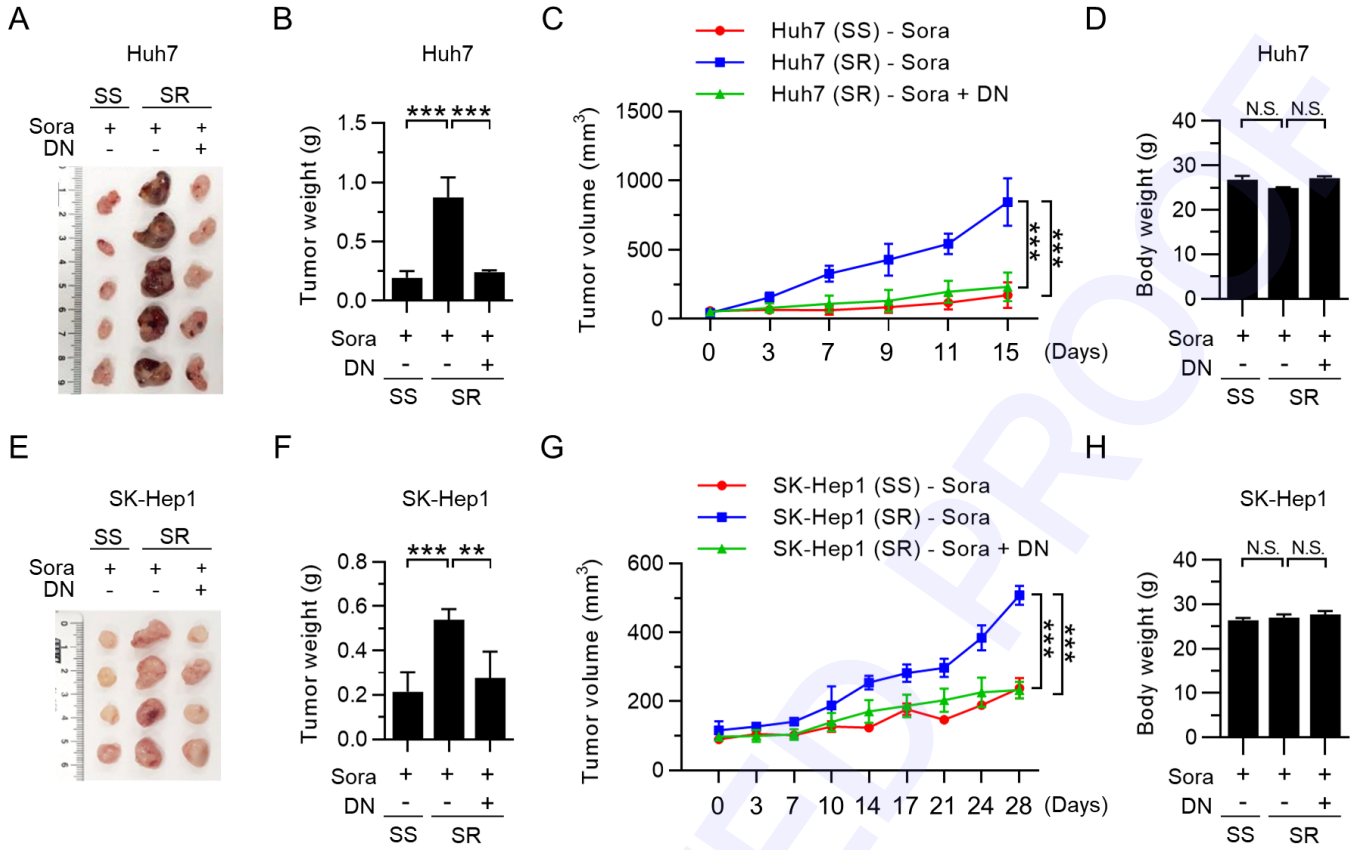

Fig. 4. Revised Figure 4